Article:

Kesserwani, G., Shamkhalchian, A. and Zadeh, M.J. (2014) Fully coupled discontinuous galerkin modeling of dam-break flows over movable bed with sediment transport. Journal of Hydraulic Engineering, 140 (4). 06014006. ISSN 0733-9429

https://doi.org/10.1061/(ASCE)HY.1943-7900.0000860

Fully-coupled discontinuous Galerkin modelling of dam-break flows over movable bed with sediment transport

Georges Kesserwani[1], Alireza Shamkhalchian[2]and Mahboobeh Jomeh Zadeh[3]

Abstract

A one-dimensional (1D) discontinuous Galerkin morphodynamic model has been devised with application to simulate of dam-break flows over erodible beds with suspended sediment transport. The morphodynamic equations adopt the shallow water equations (SWE) considering the interaction of sediment transport and bed changes on the flow. A local second-order Runge-Kutta discontinuous Galerkin (RKDG2) model has been reformulated to numerically solve the morphodynamic equations in a fully-coupled manner and with a non-capacity sediment model. The model's implementation is thoroughly detailed with focus on the discretization of the complex source terms, the treatment of wetting and drying, and other stabilizing issues pertaining to high solution gradients and the transient character of the topography. The model has been favorably applied to replicate experimental dam-break flow over erodible sediment beds.

Key-words: Dam-break flows; Discontinuous Galerkin; erodible beds; sediment transport; complex source terms; wetting and drying; model testing.

[1]Lecturer, Pennine Water Group, Civil and Structural Engineering, The University of Sheffield, Mappin St., Sheffield S1 3JD, UK (corresponding author). Email: g.kesserwani@sheffield.ac.uk

[2]MSc Student, Civil Engineering Department, Ferdowsi University of Mashhad, Wakil Abad Blvd., Mashhad, PO Box 91775-1111, Iran. Email: shamkhalchian_alireza@yahoo.com

[3]MSc Student, Civil Engineering Department, Ferdowsi University of Mashhad, Wakil Abad Blvd., Mashhad, PO Box 91775-1111, Iran. Email: mahboobeh_jomezadeh@yahoo.com

Introduction

Modelling shallow water flows over mobile topographies is useful to study hydraulic engineering problems involving dam break, river, canal and coastal hydrodynamics. For turbulent flows over erodible sediment beds, such as the first instants of a dam-break wave, the sediment concentration is so high and the bed topography changes rapidly that their effects on the flow dynamics cannot be ignored, and thus the entire morphodynamic process needs to be incorporated in the simulation (Forman et al. 2007, El Kadi Abederrezak and Paquier 2009, Pasquale et al. 2011, Ali et al. 2012, Cao et al. 2012).

A mathematical morphodynamics model is commonly achieved by joining the Exner equation, taken with a model for sediment transport, to the depth-averaged shallow water equations (SWE). Numerical approaches for solving the resulting set of equations can be coupled or decoupled, and with capacity or non-capacity sediment transport relationship (Cao et al. 2002, Wu et al. 2004, Wu (2007), El Kadi Abderrezak and Paquier 2011, Cao et al. 2012). Here, the fully-coupled model philosophy of Cao et al. (2004), with non-capacity sediment, is considered within the focus of formulating a new hydro-morphodynamic model based on the Discontinuous Galerkin (DG) method.

In recent years, the class of finite volume Godunov-type methods solving the SWE (Toro and García-Navarro 2007) has been extended to solve the fully-coupled morphodynamic equations. Cao et al. (2004) used the HLLC Riemann solver providing reasonable level of modelling for fluvial processes over erodible beds. A more comprehensive model was later devised by Wu and Wang (2007) in which a correction factor was introduced to the sediment model. More recently, efforts have been made to extend second-order hydrodynamic models to resolve the fully-coupled morphodynamic equations (Xia et al. 2010, Li and Duffy 2011, Li et al. 2013). Despite this progress, the discretizations issues particular to ad-hoc treatment of complex source terms, wetting and drying, and high-order slopes, relative to context of morphological modelling, seems to be somewhat overlooked. In this context, Benkhaldoun et al. (2012) studied slope-limiting issues suggesting the further need to limit the slope components involved in the bed-evolution to maintain stability. Li et al. (2013) concluded that the accuracy of second-order hydromorphological models is likely to be compromised if no special treatment to the irregular topography is further considered. Certainly, the reliability of a fully-coupled morphodynamic numerical model is further dependent on its further ability to handle wet/dry fronts along with the complex source terms. These are desirable features to possess within the design of a second-order accurate hydro-morphodynamic numerical model, which is the purpose of this work on the subject of an extension to a well-established RKDG2 (second-order Runge-Kutta [RK] DG) hydrodynamic solver (Kesserwani and Liang 2012b).

The DG method conceptually extends the local finite volume method to arbitrary order of accuracy, is locally conservative and highly suited for coarse mesh simulations (Cockburn and Shu 2001, Kesserwani 2013). The DG has become quite developed for modelling hydrodynamics supported by the latest advances in computational hydraulics such as accurate integration of irregular topographies, localized Total Variation Diminishing (TVD) slope liming, and polynomial wet/dry front tracking (Buyna et al. 2010, Xing et al. 2010, Kesserwani and Liang 2012a; Lai and Khan 2012). As to the hydro-morphodynamic modelling, applications of the DG method are quite few and only considered bed-load sediment transport, wet domains and smooth flow simulations (Tassi et al. 2008; Mirabito et al. 2011). To the best of the writers' knowledge, the DG method has not yet been: (i) formulated for solving the fully-coupled morphodynamic equations with non-capacity suspended sediment model, and (ii) applied to solve dam-break flows over movable sediment beds.

This paper newly explores issues (i) and (ii) within an RKDG2 solver. The technical formulation of the RKDG2 hydro-morphodynamic model is presented including all key discretization details relevant to topography and sediment source terms, treatment of wetting and drying, and stabilization of the morphodynamic numerical solution. The model's performance is tested and discussed for two experimental dam-break flows scenarios involving bed-erosion and sediment-transport. Finally, results are summarized and conclusions are drawn.

Hydro-morphodynamic model

The 1D SWE coupled with the Exner equation including a sediment transport model may be cast in the following conservative form (Cao et al. 2004, Li and Duffy 2011):

$$\frac{\partial \mathbf{U}}{\partial t} + \frac{\partial \mathbf{F}(\mathbf{U})}{\partial x} = \mathbf{S} \tag{1}$$

$$\mathbf{U} = \begin{pmatrix} h \\ hu \\ h\Psi \\ \Phi \end{pmatrix} \text{ and } \mathbf{F}(\mathbf{U}) = \begin{pmatrix} hu \\ hu^2 + \frac{g}{2}h^2 \\ hu\Psi \\ hu\Psi \end{pmatrix} \tag{2}$$

t = time (s), x = space coordinate (m),.**U**, **F**(**U**) and **S** are, respectively, vectors containing the conserved variables, the fluxes and the source terms, in which h = water depth (m), u = flow velocity (m/s), g= gravitational acceleration (m/s^2), Ψ = flux-averaged volumetric sediment concentration (m^3/m^3) and Φ is a factor representing the bed evolution that may be expressed in terms of bed porosity p and the bed elevation z (m):

$$\Phi = (1-p)z + (h\Psi) \tag{3}$$

Assuming that there is no precipitation and infiltration, the suspended load is dominant over the bed load, and constant roughness, the vector of source terms may be decomposed as sum of topography source term, friction source term, the suspended-load sediment concentration variation and the sediment exchange, which are respectively denoted by $\mathbf{S_0}$, $\mathbf{S_f}$, $\mathbf{S_c}$ and $\mathbf{S_e}$, i.e.

$$\mathbf{S} = \mathbf{S_0} + \mathbf{S_f} + \mathbf{S_c} + \mathbf{S_e} \tag{4}$$

with,

$$\mathbf{S_0} = \begin{pmatrix} 0 \\ ghs_0 \\ 0 \\ 0 \end{pmatrix}, \mathbf{S_f} = \begin{pmatrix} 0 \\ -C_f|u|u \\ 0 \\ 0 \end{pmatrix}, \mathbf{S_c} = \begin{pmatrix} 0 \\ -\frac{(\rho_s-\rho_w)gh^2}{2\rho}\frac{\partial \Psi}{\partial x} \\ 0 \\ 0 \end{pmatrix}, \text{ and } \mathbf{S_e} = \begin{pmatrix} \frac{E-D}{1-p} \\ -\frac{(\rho_z-\rho)(E-D)u}{\rho(1-p)} \\ E-D \\ 0 \end{pmatrix} \tag{5}$$

In which, $s_0 = -\partial z/\partial x$ = bed slope, $C_f = g{n_m}^2/h^{1/3}$ = friction factor (with n_m = Manning coefficient); p = bed sediment porosity, ρ_w = density of water, ρ_s = density of sediment, and ρ and ρ_z are water-sediment mixture density and saturated bed density, respectively, which are related as:

$$\rho = \rho_w(1-\Psi) + \rho_s\,\Psi \text{ and } \quad \rho_z = \rho_w p + \rho_s(1-p) \tag{6}$$

Within $\mathbf{S_e}$, E and D represent sediment entertainment and deposition fluxes, which can be obtained by different empirical formulas (Fagherazzi and Sun 2003, Cao et al. 2004, El Kadi Abederrezak and Paquier 2011, Li and Duffy 2011, Cao et al. 2012). Herein, the following expression for E and D are selected (Li and Duffy 2011):

$$E = \alpha(\theta - \theta_c)h|u| \text{ and } D = \beta\Psi\omega \tag{7}$$

Where, α = given calibration constant, θ_c = critical shields factor for starting of sediment particles movement, and θ is evaluated as $\theta = {u_*}^2/\,gsd$ where $u_* = \sqrt{C_f u^2}$ = friction velocity, d = sediment particle diameter and $s = \rho_s/\rho_w - 1$ is the submerged specific gravity; $\beta = \min[2\,,(1-p)/\Psi]$, ω = velocity of the sediment particles, which is given by $\omega = \sqrt{(13.95\nu/d)^2 + 1.09gsd} - 13.95\nu/d$ with ν = kinematic viscosity of water.

Discontinuous Galerkin method

The conceptual underpinning of local DG method for solving the hyperbolic conservation laws is mainly attributed to Cockburn and Shu (2001). Here, the technical focus is mainly devoted to the extension of a valid RKDG2 scheme solving the SWE to further solve the hydro-morphodynamic system (1).

RKDG2 formulation

A 1D computational domain [x_{min}, x_{max}] is subdivided into N uniform cells I_i = [$x_{i-1/2}$; $x_{i+1/2}$], each centred at x_i= ($x_{i+1/2}$ + $x_{i-1/2}$)/2 of length Δx = $x_{i+1/2}$ -$x_{i-1/2}$. The RKDG2 framework seeks a local linear approximate solution $\mathbf{U_h}$ that is spanned by two local coefficients $\mathbf{U}_i^0(t)$ and $\mathbf{U}_\mathrm{i}^1(t)$ and can be expanded as:

$$\mathbf{U_h}(x,t)|_{I_i} = \mathbf{U}_i^0(t) + \mathbf{U}_i^1(t)\,\frac{(x-x_i)}{\Delta x/2} \qquad (\forall x \in I_i) \tag{8}$$

The initial coefficients are polynomial projections to the initial condition $\mathbf{U}_0(x) = \mathbf{U}(x,0)$ and may be written as (Kesserwani et al. 2010):

$$\mathbf{U}_i^0(0) = \int_{x_{i-1/2}}^{x_{i+1/2}} \mathbf{U}_0(x)dx \approx \frac{1}{2}\left[\mathbf{U}_0\left(x_{i+1/2}\right) + \mathbf{U}_0\left(x_{i-1/2}\right)\right] \tag{9}$$

$$\mathbf{U}_i^1(0) = \int_{x_{i-1/2}}^{x_{i+1/2}} \mathbf{U}_0(x)\left(\frac{x-x_i}{\Delta x}\right)dx \approx \tfrac{1}{2}\left[\mathbf{U}_0\left(x_{i+1/2}\right) - \mathbf{U}_0\left(x_{i-1/2}\right)\right] \quad (10)$$

The semi-discrete DG transformation to the conservative form (1) produces two sets of independent ODEs for the spatial update of the local coefficients

$$\frac{d}{dt}\begin{pmatrix}\mathbf{U}_i^0(t) & 0 \\ 0 & \mathbf{U}_i^1(t)\end{pmatrix} = \begin{pmatrix}\mathbf{L}_i^0 & 0 \\ 0 & \mathbf{L}_i^1\end{pmatrix} \quad (11)$$

$\mathbf{L}_i^0$ and $\mathbf{L}_i^1$ are local space operators obtained by the DG discretization (Kesserwani and Liang 2011):

$$\mathbf{L}_i^0 = -\frac{1}{\Delta x}\left[\tilde{\mathbf{F}}_{i+1/2} - \tilde{\mathbf{F}}_{i-1/2}\right] + \mathbf{S}_{|I_i}(\mathbf{U}_i^0) \quad (12)$$

$$\mathbf{L}_i^1 = -\frac{3}{\Delta x}\left\{\tilde{\mathbf{F}}_{i+\frac{1}{2}} + \tilde{\mathbf{F}}_{i-\frac{1}{2}} - \mathbf{F}_{|I_i}\left(\boldsymbol{U}_i^0 + \frac{\widehat{\boldsymbol{U}}_i^1}{\sqrt{3}}\right) - \mathbf{F}_{|I_i}\left(\boldsymbol{U}_i^0 - \frac{\widehat{\boldsymbol{U}}_i^1}{\sqrt{3}}\right) - \frac{\sqrt{3}\Delta x}{6}\left[\mathbf{S}_{|I_i}\left(\boldsymbol{U}_i^0 + \frac{\widehat{\boldsymbol{U}}_i^1}{\sqrt{3}}\right) - \mathbf{S}_{|I_i}\left(\boldsymbol{U}_i^0 - \frac{\widehat{\boldsymbol{U}}_i^1}{\sqrt{3}}\right)\right]\right\} \quad (13)$$

$\mathbf{S}$ contains all the source terms in (4) excluding $\mathbf{S_f}$. The "hat" symbol over a slope coefficient refers to the controlled slope coefficient due to the local slope-limiting process. The inter-cells fluxes, e.g. $\tilde{\mathbf{F}}_{i+1/2}$ at interface $x_{i+1/2}$ shared by neighbouring cells I_i and I_{i+1}, are obtained by solving the local Riemann problem, defined by the solution's at interface $x_{i+1/2}$:

$$\mathbf{U}_{i+1/2}^- = \mathbf{U_h}(x_{i+1/2}^-, t)\Big|_{I_i} = \mathbf{U}_i^0 + \widehat{\mathbf{U}}_i^1 \quad (14)$$

$$\mathbf{U}_{i+1/2}^+ = \mathbf{U_h}(x_{i+1/2}^+, t)\Big|_{I_{i+1}} = \mathbf{U}_{i+1}^0 - \widehat{\mathbf{U}}_{i+1}^1 \quad (15)$$

The numerical flux $\tilde{\mathbf{F}}_{i+1/2} = \tilde{\mathbf{F}}\left(\mathbf{U}_{i+1/2}^-, \mathbf{U}_{i+1/2}^+\right)$ is evaluated based on the HLL Riemann solver (Toro et al. 1994). Finally, the two local coefficients are lifted to the next time level via the two-stage explicit RK time method:

$$\left(\mathbf{U}_i^{0,1}\right)^{n+1/2} = \left(\mathbf{U}_i^{0,1}\right)^n + \Delta t\left(\mathbf{L}_i^{0,1}\right)^n \quad (16)$$

$$(\mathbf{U}_i^{0,1})^{n+1} = \tfrac{1}{2}\left[(\mathbf{U}_i^{0,1})^n + (\mathbf{U}_i^{0,1})^{n+1/2} + \Delta t\left(\mathbf{L}_i^{0,1}\right)^{n+1/2}\right] \quad (17)$$

Theoretically, the RKDG2 time step is restricted by the Courant-Friedrichs-Lewy (CFL) condition, with a Courant number smaller than 0.333 (Cockburn and Shu 2001). However our convergence study, considering both aspects of mesh-size and slope-limiting, shows that the RKDG2 morphodynamic numerical model requires a more restrictive time step – Courant number equal to 0.1 – to avoid numerical instability that may occur in resolution of the mobile topography. This restriction has also been reported for finite volume hydro-morphodynamic models (Li and Duffy 2011, Benkhaldoun et al. 2012).

Discretization of the source terms

- Friction source term ($\mathbf{S_f}$): to avoid possible numerical instability near dry zones with high roughness, the friction source term is commonly discretised by a splitting implicit approach prior to time stage and step, i.e. not included explicitly within the space operators $\mathbf{L}_i^0$ and $\mathbf{L}_i^1$; see Kesserwani and Liang 2012a for technical details.
- Sediment exchange source term ($\mathbf{S_e}$): is discretized explicitly and via direct local calculation of E and D evaluated using the local coefficients relative to the approximate variables h_h, $(hu)_h$, Ψ_h and Eq. (7).
- Sediment concentration variations source term ($\mathbf{S_c}$): is discretized explicitly but requires specific mathematical and numerical treatment to cope with the gradient of the sediment concentration. That is, the second term of the vector $\mathbf{S_c}$ is first rewritten as:

$$-\frac{(\rho_s-\rho_w)gh^2}{2\rho}\frac{\partial\Psi}{\partial x} = -\frac{(\rho_s-\rho_w)g}{2\rho}h^2\left(\frac{\partial\left(\frac{h\Psi}{h}\right)}{\partial x}\right) = -\frac{(\rho_s-\rho_w)g}{2\rho}\left[h\frac{\partial(h\Psi)}{\partial x} - h\Psi\frac{\partial h}{\partial x}\right] \qquad (18)$$

and is then locally discretized as:

$$\left[-\frac{(\rho_s-\rho_w)gh^2}{2\rho}\frac{\partial\Psi}{\partial x}\right]_{I_i} \approx -\frac{(\rho_s-\rho_w)g}{2\rho}\left[h_h\frac{\partial(h\Psi)_h}{\partial x} - (h\Psi)_h\frac{\partial h_h}{\partial x}\right] \qquad (19)$$

With

$$\left[\frac{\partial(h\Psi)_h}{\partial x}\right]_{I_i} = \frac{\partial}{\partial x}\left[(h\Psi)_i^0 + \left(\frac{x-x_i}{\Delta x/2}\right)(h\Psi)_i^1\right] = \frac{(h\Psi)_i^1}{\Delta x/2} \qquad (20)$$

$$\left[\frac{\partial h_h}{\partial x}\right]_{I_i} = \frac{\partial}{\partial x}\left[h_i^0 + \left(\frac{x-x_i}{\Delta x/2}\right)h_i^1\right] = \frac{h_i^1}{\Delta x/2} \qquad (21)$$

- Topography source term ($\mathbf{S_0}$): is locally discretized in a well-balanced manner (Kesserwani et al. 2010) by:

$$z_h(x,t)|_{I_i} = \mathrm{z}_i^0(t) + z_i^1(t)\frac{(x-x_i)}{\Delta x/2} \qquad (\forall x \in I_i) \qquad (22)$$

With $z_i^0(t)$ and $z_i^1(t)$ are topography-associated coefficients, which may be initially produced following similar (scalar) relationships as in (9) and (10). With this, the bed slope term, s_0, is locally discretized as:

$$[s_0]_{I_i} = \left[-\frac{\partial z_h(x,t)}{\partial x}\right]_{I_i} = -\frac{\partial}{\partial x}\left[z_i^0(t) + \left(\frac{x-x_i}{\Delta x/2}\right) z_i^1(t)\right] = -\frac{z_i^1(t)}{\Delta x/2} \quad (23)$$

Wetting and drying condition

Prior to evaluation the operators $\mathbf{L}_i^0$ and $\mathbf{L}_i^1$, the local coefficients, $\mathbf{U}_i^0(t)$ and $\mathbf{U}_i^1(t)$, are revisited to ensure the positivity of the water depth in the calculation of the inter-cells fluxes, the local fluxes and the source terms. The action of the wetting and drying for the current hydro-morphodynamic model is summarized in steps below:

1. Reconstruct the free-surface elevation, η = h + z, limits at interface $x_{i+1/2}$ using relationships (14) and (15): $\eta_{i+1/2}^- = \left(h_i^0 + z_i^0\right) + (\widehat{h_i^1 + z_i^1})$ and $\eta_{i+1/2}^+ = \left(h_{i+1}^0 + z_{i+1}^0\right) - (\widehat{h_{i+1}^1 + z_{i+1}^1})$.
2. Evaluate the limits of the discharge components in $\mathbf{U_h}$ at interface $x_{i+1/2}$: $(hu)_{i+1/2}^- = (hu)_i^0 + \widehat{(hu)}_i^1$, $(h\Psi)_{i+1/2}^- = (h\Psi)_i^0 + \widehat{(h\Psi)}_i^1$, $(hu)_{i+1/2}^+ = (hu)_{i+1}^0 - \widehat{(hu)}_{i+1}^1$, $(h\Psi)_{i+1/2}^+ = (h\Psi)_{i+1}^0 - \widehat{(h\Psi)}_{i+1}^1$.
3. Evaluate the limits of the topography z at interface $x_{i+1/2}$: $z_{i+1/2}^- = z_i^0 + z_i^1$, $z_{i+1/2}^+ = z_{i+1}^0 - z_{i+1}^1$; accordingly estimate the limits of Φ using Eq. (3): $\Phi_{i+1/2}^K = (1-p)z_{i+1/2}^K + (h\Psi)_{i+1/2}^K$, $(K = +,-)$.
4. Calculate the limits of the velocity and sediment concentration variables at interface $x_{i+1/2}$: $u_{i+1/2}^K = (hu)_{i+1/2}^K / h_{i+1/2}^K$ and $\Psi_{i+1/2}^K = (h\Psi)_{i+1/2}^K / h_{i+1/2}^K$ with $h_{i+1/2}^K = \eta_{i+1/2}^K - z_{i+1/2}^K$ $(K = +,-)$.
5. Now apply the topography discretization, at interface $x_{i+1/2}$, along with wetting and drying:
    a. Re-define numerically the topography limits: $z_{i+1/2}^{K,*} = \eta_{i+1/2}^K - h_{i+1/2}^K$ $(K = +,-)$.
    b. Set a single z-value $z_{i+1/2}^{\pm,*}$ defined by the maximum: $z_{i+1/2}^{\pm,*} = \max(z_{i+1/2}^{-,*}, z_{i+1/2}^{+,*})$.
    c. Preserve the positivity of the water depth: $h_{i+1/2}^{K,*} = \max(0, \eta_{i+1/2}^K - z_{i+1/2}^{\pm,*})$ $(K = +,-)$.
    d. Find the flow and sediment discharges incorporating the original velocities and sediment concentration, i.e. $(hu)_{i+1/2}^{K,*} = h_{i+1/2}^{K,*} u_{i+1/2}^K$ and $(h\Psi)_{i+1/2}^{K,*} = h_{i+1/2}^{K,*} \Psi_{i+1/2}^K$, and the free-

surface elevation, i.e. $\eta_{i+1/2}^{K,*} = h_{i+1/2}^{K,*} + z_{i+1/2}^{\pm,*}$, associated with the positivity-preserving water depth and the single value of the topography.

e. Ensure that step 5-c does not cancel the actual water level at a wet/dry front (Liang 2010):

   i. Calculate $\Delta\eta_{i+1/2} = \max\left[0, -\left(\eta_{i+1/2}^{-} - z_{i+1/2}^{\pm,*}\right)\right]$ (during step 5-c).

   ii. Adjust $\eta_{i+1/2}^{K,*} \leftarrow \eta_{i+1/2}^{K,*} - \Delta\eta_{i+1/2}$ and $z_{i+1/2}^{\pm,*} \leftarrow z_{i+1/2}^{\pm,*} - \Delta\eta_{i+1/2}$ $(K = +,-)$.

6. Calculate the flux $\tilde{\mathbf{F}}_{i+1/2}$ at interface $x_{i+1/2}$ using $\mathbf{U}_{i+1/2}^{K}$ incorporating the depth-positivity-variables $h_{i+1/2}^{K,*} = \eta_{i+1/2}^{K,*} - z_{i+1/2}^{\pm,*}$, $h_{i+1/2}^{K,*} u_{i+1/2}^{K}$ and $h_{i+1/2}^{K,*} \Psi_{i+1/2}^{K}$ $(K = +,-)$.

7. Repeat steps 1-6 to evaluate the flux $\tilde{\mathbf{F}}_{i-1/2}$ at interface $x_{i-1/2}$.

8. Redefine the local coefficients of the main variables to comply with the action of wetting and drying, i.e. $\bar{z}_i^0 = (z_{i+1/2}^{\pm,*} + z_{i-1/2}^{\pm,*})/2$, $\bar{z}_i^1 = (z_{i+1/2}^{\pm,*} - z_{i-1/2}^{\pm,*})/2$; $\bar{h}_i^{0,1} = \bar{\eta}_i^{0,1} - \bar{z}_i^{0,1}$ with $\bar{\eta}_i^0 = (\eta_{i+1/2}^{-,*} + \eta_{i-1/2}^{+,*})/2$ and $\bar{\eta}_i^1 = (\eta_{i+1/2}^{-,*} - \eta_{i-1/2}^{+,*})/2$; $(\overline{hu})_i^0 = [(hu)_{i+1/2}^{-,*} + (hu)_{i-1/2}^{+,*}]/2$ and $(\overline{hu})_i^1 = [(hu)_{i+1/2}^{-,*} - (hu)_{i-1/2}^{+,*}]/2$; $(\overline{h\Psi})_i^0 = [(h\Psi)_{i+1/2}^{-,*} + (h\Psi)_{i-1/2}^{+,*}]/2$ and $(\overline{h\Psi})_i^1 = [(h\Psi)_{i+1/2}^{-,*} - (h\Psi)_{i-1/2}^{+,*}]/2$; then use them to evaluate the local fluxes and source terms within the local space operators (12) and (13).

Local slopes control

To avoid spurious oscillations that would probably occur around discontinuous local solutions, the TVD minmod limiter is applied to control the variation of the local slope coefficient $\mathbf{U}_i^1$ (Toro 2001). Within DG methods, the slope limiter needs to be localized to those troubled-slope components. Herein, the same local slope-limiting strategy used within the RKDG2 hydrodynamic model has been applied to the variables of the morphodynamic model, namely in a component-wise manner and after normalization. Slope-limiting is deactivated around cells involving a wet/dry front to avoid unnecessary instabilities (Kesserwani and Liang 2012b). After the slope monitoring process, a local slope coefficient is denoted by $\widehat{\mathbf{U}}_i^1$ regardless of whether it has been limited or not.

Transient topography update

While completing wetting and drying along with source terms discretization, the local topography-associated coefficients are extracted explicitly after each time step and inner time stage:

- At t = n, coefficients $(z_i^0)^n$ and $(z_i^1)^n$ are either initially available, i.e. when n = 0, or reset, i.e. $(z_h|_{I_i})^n = (z_h|_{I_i})^{n+1}$. These coefficients are used in the topography discretization with wetting and drying to calculate the space operators $(\mathbf{L}_i^{0,1})^n$, and thereby move the local solution to the intermediate stage n + ½, via Eq. (16).
- At t = n + ½, $(\mathbf{L}_i^{0,1})^{n+1/2}$ is evaluated using new topography coefficients, i.e. $(z_i^0)^{n+1/2}$ and $(z_i^1)^{n+1/2}$, which are obtained from the intermediate solution variables by means of Eq. (3):

$$(z_h|_{I_i})^{n+1/2} = \left[\frac{\Phi_h|_{I_i} - (h\Psi)_h|_{I_i}}{1-p}\right]^{n+1/2} \tag{24}$$

- After the second RK stage, the two coefficients spanning $z_h(x,t)$ are updated again, using Eq. (3), according to the solution's variables at the next time level t = n + 1:

$$(z_h|_{I_i})^{n+1} = \left[\frac{\Phi_h|_{I_i} - (h\Psi)_h|_{I_i}}{1-p}\right]^{n+1} \tag{25}$$

Model testing

The RKDG2 scheme solving the hydrodynamic equations with fixed beds has been well tested for benchmark tests involving irregular topographies, high friction effects, water jumps and wetting and drying (Kesserwani and Liang 2010, 2011, 2012a,b). The purpose here is to retest these abilities for the new RKDG2 hydro-morphodynamic solver, and, meanwhile, illustrate its performance in modelling dam-break waves over erodible beds with sediment transport. The present model is validated for two small-scale experimental tests characterized by an initially flat sediment beds.

The current RKDG2 model is applied to reproduce the dam-break experiments carried out in Taipei and Louvain (Capart and Young 1998, Fraccarollo and Capart 2002), respectively. Both experiments were conducted in horizontal prismatic flumes of rectangular cross-sections, but primarily differ in the sediment materials used. The flume in the Taipei experiment was 1.2 m long, 0.2 m wide and 0.7 m high. It was initially covered by a 5-6 cm thick layer of light artificial pearls, of a diameter of 6.1 mm, specific gravity of 1.048 and settling velocity of 0.076 m/s. In the Louvain experiment, the flume was 2.5 m long, 0.1 m wide and 0.35 m high. Cylindrical PVC pellets having a diameter of 3.2 mm, height of 2.8 mm (an equivalent spherical diameter of 3.5 mm), specific gravity of 1.54, and settling velocity of 0.18 m/s constituted an initial sediment layer of 5-6 cm thick over the fixed bottom. In both experiments, a dam was located in the middle of the flume separating an upstream static flow region of 10 cm deep from the dry downstream part. At t = 0 s, the dam was lifted rapidly to create the dam-break flow over the flat beds. In both of the tests, the flow (hu) and sediment discharges ($h\Psi$), and the bed evolution parameter (Φ) are initialized to zero, while the water level is assumed to be initially discontinuous:

$$h(x,0) = \begin{cases} 0.1 & (x < 0) \\ 0 & (x \geq 0) \end{cases} \tag{26}$$

The bed porosity is set to 0.28 and 0.3 for the Taipei test and the Louvain test, respectively, while a Manning roughness $n_m = 0.025\ \mathrm{s/m^{1/3}}$ and a water density of $\rho_w = 1\ \mathrm{g/cm^3}$ are used for both (Li and Duffy 2011). According to the critical shields curve, in Cao et al. (2006), the parameter θ_c is estimated to be (roughly) less than 0.076 for grained sediments with a diameter range between 3.5 mm and 6.1 mm. However, past literature point out the use of higher values for θ_c for these tests. For example, Li and Duffy (2011) and Li et al. (2013) directly used a higher θ_c (= 0.15 for the Louvain case) obtained by calibration, whereas Wu and Wang (2007) introduced a correction factor, that (indirectly) amends θ_c. In this work, parameters α and θ_c were calibrated; two sets of parameters $\{\alpha, \theta_c\}$ are selected and explored for each test, which are {2.5, 0.05} and {2.2, 0.12} for the Taipei test, and {4, 0.05} and {2.5, 0.05} for the Louvain test. Pseudo-analytical free-surface and bed elevations maybe derived based on a number of assumptions (Fraccarollo and Capart 2002). The domains were divided into 100 cells and the simulation time is 0.6 s and 1.2 s for the Taipei and the Louvain tests, respectively, which were non-dimensionalized according to $t_0 = \sqrt{g/h_0} \approx 0.101$ ($h_0 = 0.1$). Transmissive boundary conditions are configured during the simulations, for completeness, although the flow does not reach boundaries. Fig. 1 compares the predicted free-surface and bed evolutions, at three successive output times, with the pseudo-analytical profiles and the measurements for the Taipei (Fig. 1 - left panel) and Louvain (Fig. 1 - right panel) tests.

For the Taipei test, the numerical model is seen to underestimate the erosion upstream of the scour hole which is, however, overestimated by the pseudo-analytical bed solution, as compared to the measurement. The hydraulic jump, aligned with the bed erosion, is successfully predicted by the RKDG2 model. Despite being a bit faster than the experimental jump profile, the RKDG2 model's localization to the jump matches the results of alternative finite volume models published in literature (Wu and Wang 2007, Li and Duffy 2011, Li et al. 2013). The disagreements amongst the pseudo-analytical, numerical and experimental profiles are expected and their causes have been reported previously (Capart and Young 1998; Fraccarollo and Capart 2002, Li and Duffy 2011, Li et al. 2013). Relating to the sediment parameters $\{\alpha,\ \theta_c\}$, as reflects Fig. 1 (left panel) the choice {2.5, 0.05}, incorporating $\theta_c < 0.076$, appears to be more appropriate for this test.

For the Louvain test, the depth and bed profiles simulated by the RKDG2 model are displayed at the right panel in Fig. 1 revealing a more satisfactory agreement between the computed, pseudo-analytical and measured results than for the Taipei test. In this test, at $t = 10t_0$, the RKDG2 model provides a better prediction to the hydraulic jump relating to the measurements, and is able to locate well the position of the wave front and the erosion magnitude albeit showing a clear underestimation to the latter for the choice {2.5, 0.05} to the initial sediment parameters. In contrast, the RKDG2 predictions relative to the choice {4.0, 0.05} appear to capture both the analytical and experimental erosion extent with greater qualitative-accuracy; thus the second choice seems to be more appropriate for the Louvain test. Expectedly, the analytical solution excludes the hydraulic jump and tends to excessively overestimates the wave front at $t = 10t_0$ (Wu and Wang 2007, Li and Duffy 2011, Li et al. 2013).

Fig. 2 illustrates the sediment concentration profiles reproduced by the numerical model at different output times for the Taipei (left panel) and Louvain (right panel) tests, respective to the sediment parameters {2.5, 0.05} and {4.0, 0.05}. From these qualitative results, it appears that the present RKDG2 model is capable to represent high sediment concentrations with no sign of instability around steep sediment gradient under relatively strong (initial) erosive conditions. The RKDG2 sediment predictions relative to the other selected choices of parameters $\{\alpha, \theta_c\}$ are quite similar to the predictions available in Fig. 2 and are, therefore, not illustrated further. The present RKDG2 predictions to the sediment concentration profiles match closely those predicted by alternative finite volume formulations reported in literature (Wu and Wang 2007, Li and Duffy 2011, Li et al. 2013) demonstrating the capability of the extended RKDG2 numerical model to deliver highly accurate and stable prediction to sediment concentration peaks along with the occurrence of wet/dry front, bed erosion and shock development.

Conclusions

This work addressed 1D modelling of dam-break flow over movable sediment beds particular to the framework of a second-order Runge-Kutta Discontinuous Galerkin method (RKDG2). The RKDG2 method was reformulated to solve the fully-coupled set of hydro-morphodynamic equations and including the interaction between sediment concentration and bed change on the flow. The extended RKDG2 model was reinforced with all necessary technical ingredients for handling steep solution gradients, wetting and drying, and complex source terms. The new RKDG2 morphodynamic formulation was applied to replicate experimental water-surface and bed-evolution data corresponding to two dam-break scenarios in which the wave breaks over an initially flat and dry sediment bed.

Numerical evidences demonstrate that the RKDG2 fully-coupled morphodynamic model is able to concurrently predict the changes occurring in the water flow, the bed-evolution and the concentration of suspended sediments with reasonable precision comparing to either the available experiments and/or alternative simulation published in literature. Our testing suggest that the present RKDG2 morphodynamic formulation is valid for simulation of complex shallow flow processes including water jumps, wetting and drying, irregular bed evolution and suspension of sediments. Nevertheless, its applicability seems to be highly dependent on appropriate selection and/or calibration to the sediment parameters for a specific configuration. Two-dimensional extension to the RKDG2 morphodynamic model is feasible and this work constitutes the gateway for it.

List of figure legends

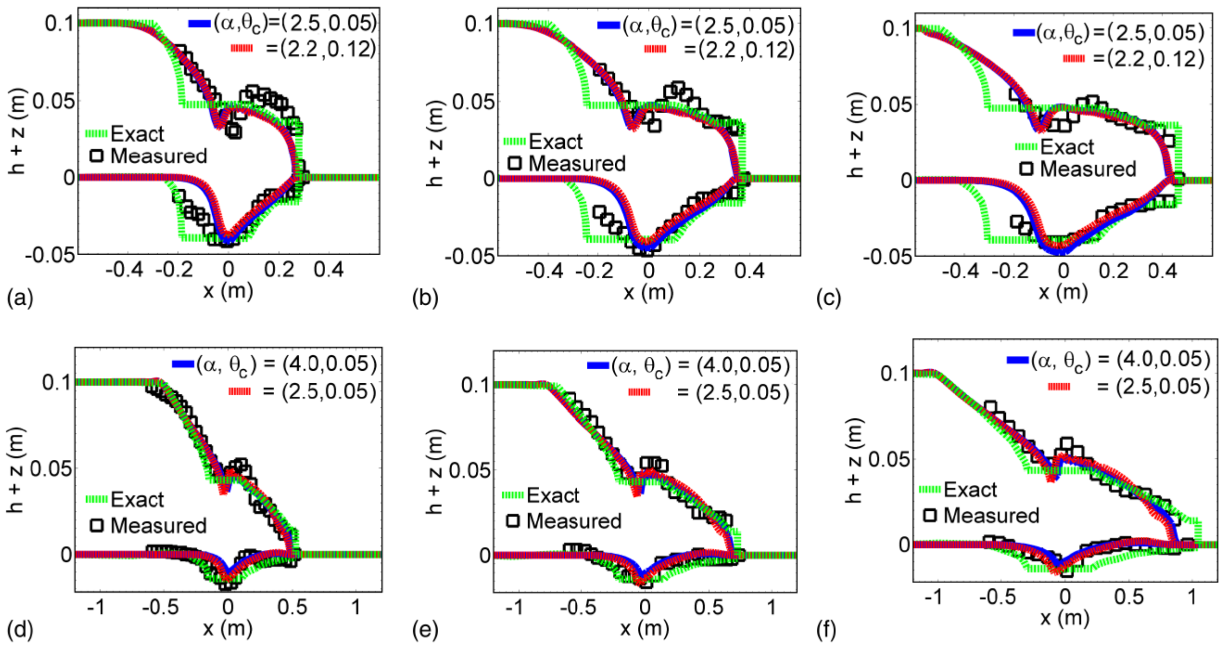

Fig. 1 water and bed surface RKDG2 predictions compared with the experimental and pseudo-analytical solutions at three successive output times. <u>Left panel:</u> Taipei test results at time $3t_0$, $4t_0$ and $5t_0$ (respectively from top to end); <u>Right panel:</u> Louvain test results at time $5t_0$, $7t_0$ and $10t_0$ (respectively from top to end).

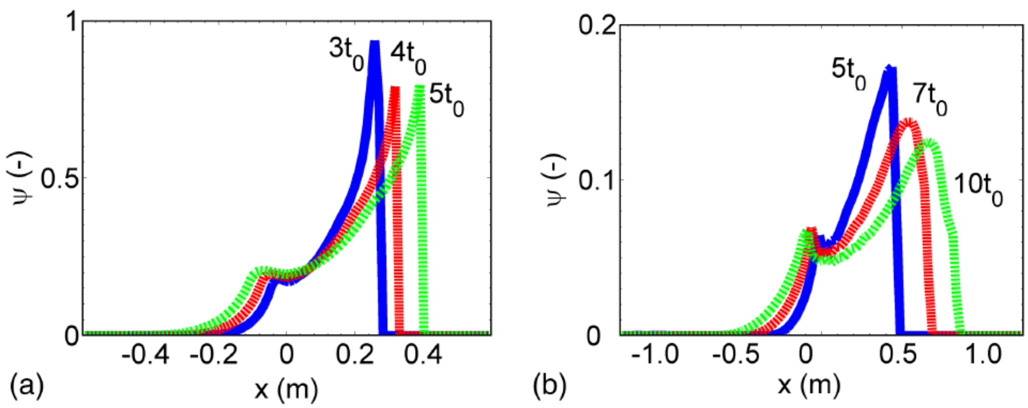

Fig. 2 sediment concentration predicted by the RKDG2 model for the Taipei (left panel) and Louvain (right panel) tests.

Notations

$\mathbf{S}$ =source terms

$\mathbf{S_0}$ =Topography source term vector

$\mathbf{S_c}$ =sediment concentration variation source term vector

$\mathbf{S_e}$ = sediment exchange source term vector

$\mathbf{S_f}$ =friction source term vector

$\mathbf{F}$ =flux

$\tilde{\mathbf{F}}$ =numerical flux

$\mathbf{U}$ =conserved variables

$\mathbf{U_h}$ =local approximate solution for $\boldsymbol{U}$

$\hat{\mathbf{U}}^{\mathbf{1}}$ =limited slope-coefficient for $\boldsymbol{U}^{\mathbf{1}}$

$\mathbf{U_i^{0,1}}$ =coefficients defining a local linear solution

$\mathbf{U}^{\pm}$ $=\boldsymbol{U_h}$ at left and right hand of interface

$\mathbf{L}^{0,1}$ = Local space operator

C_f =friction coefficient

d =sediment particle diameter

D =sediment deposition flux

E =sediment entertainment flux

g =gravitational acceleration

h =water depth

i =Cell counter

I =Local cell

$\mathbf{L}^{0,1}$ = Local space operator

m =exponent in sediment deposition

n =time level

n_m =Manning coefficient

p =bed sediment porosity

s =submerged specific gravity of sediment

s_0 =bed slope

C_f =friction coefficient

t =time

t_0 = Normalized time period

u =flow velocity

u_* =frictional velocity

x =space coordinate

z =bed elevation

$z_i^{0,1}$ =local topography coefficients

Δx =computational cell length in x-direction

Δt =computational time step

α =calibration constant

η =free-surface elevation

θ =shields factor

θ_c =critical shields factor

ν =kinematic viscosity of water

ρ =water-sediment mixture density

ρ_s =sediment density

ρ_w =water density

ρ_z =saturated bed density

Φ =bed evolution parameter

Ψ =volumetric sediment concentration

ω =setting velocity of sediment particles

Reference

Ali, M., Sterk, G., Seeger, M., Boersema, M., and Peters P. (2012). “Effect of hydraulic parameters on sediment transport capacity in overland flow over erodible beds.” Hydrol. Earth Syst. Sci., 16, 591-601.

Benkhaldoun, F., Sari, S. and Seaid, M. (2012). “A flux-limiter method for dam-break flows over erodible sediment beds.” Applied Mathematical Modelling, 36, 4847-4862.

Bunya, S., Kubatko, E. J., Westerink, J. J., and Dawson, C. (2009).“A wetting and drying treatment for the Runge-Kutta discontinuous Galerkin solution to the shallow water equations.” Comput.Meth. Appl. Mech. Eng., 198(17–20), 1548–1562.

Cao, Z., Day, R., and Egashira, S. (2002). ‘‘Coupled and decoupled numerical modeling of flow and morphological evolution in alluvial rivers.’’ J. Hydraul. Eng., 128(3), 306–321.

Cao, Z., Pender, G., Wallis, S., and Carling, P. (2004).“Computational dam-break hydraulics over erodible sediment bed.” J. Hydraul. Eng., 130(7), 689–703.

Cao, Z., Pender, G., and Meng, G. (2006). “Explicit formulation of the shields diagram for incipient motion of sediment.”, J. Hydraul. Eng., 132(10), 1097–1099.

Cao, Z., Li, Z., Pender, G. and Hu, P. (2012).“Non-capacity or capacity model for fluvial sediment transport.” Water Management, 165(4),193-211.

Capart, H., and Young, D. L. (1998).“Formation of jump by the dambreak wave over a granular bed.” J. Fluid Mech., 372, 165–187.

Cockburn, B., Shu, C.W. (2001). “Runge-Kutta discontinuous Galerkin methods for convection-dominated problems.” J. Sci. Comput. 16(3), 173–261.

El kadi Abderrezzak, K., and Paquier, A. (2009).“One-dimensional numerical modeling of sediment transport and bed deformation in open channels.” Water Resour. Res., 45, W05404, doi:10.1029/2008WR007134.

El kadi Abderrezzak, K., and Paquier, A. (2011). “Applicability of sediment transport capacity formulas to dam-break flows over movable beds” J. Hydraul. Eng., 137(2), 209–221.

Fagherazzi, S. and Sun, T. (2003).“.Numerical simulations of transportational cyclic step.”Comput.& Geosciences, 29(9), 1071-1201.

Formann, E., Habersack, H.M., Schober, St. (2007). “Morphodynamic river processes and techniques for assessment of channel evolution in Alpine gravel bed rivers.” Geomorphology, 90, 340–355.

Fraccarollo, L., and Capart, H. (2002). “Riemann wave description of erosional dam-break flows.” J. Fluid Mech., 461, 183–228.

Kesserwani, G., Liang, Q., Mosé, R., and Vazquez, J. (2010). “Well balancing issues related to the RKDG2 scheme for the shallow water equations.” Int. J. Numer. Method Fluids, 62(4), 428–448.

Kesserwani, G. and Liang, Q. (2011).“A conservative high-order discontinuous Galerkin method for the shallow water equations with arbitrary topography.” Int. J. Numer. Meth. Eng. 2011, 82, 47–67.

Kesserwani, G., Liang, Q. (2012b). “Locally limited and fully conserved RKDG2 shallow water solutions with wetting and drying.” J. Sci. Comput. 50, 120–144.

Kesserwani, G., Liang, Q. (2012a). “Influence of Total-Variation-Diminishing slope limiting on local discontinuous Galerkin solutions of the shallow water equations.” J. Hydraul. Eng., 138(2), 216–222.

Kesserwani, G. (2013). “Topography discretization techniques for Godunov-type shallow water numerical models: a comparative study.” J. Hydraul. Res.doi: 10.1080/00221686.2013.796574.

Lai, W. and Khan, A.A. (2012).“Discontinuous Galerkin method for 1D shallow water flow in nonrectangular and nonprismatic channels.” J. Hydraul. Eng., 138, 285-296.

Li, S., and Duffy, C. J. (2011). “Fully coupled approach to modeling shallow water flow, sediment transport, and bed evolution in rivers.” Water Resour. Res., 47, W03508, doi:10.1029/2010WR009751.

Li, W., Vriend, H. J., Wang, Z., and. Maren, D. S. (2013) “Morphological modeling using a fully coupled, TVD upwind-biased centered scheme.” Water Resour. Res., 47, doi: 10.1002/wrcr.20138

Mirabito, C., Dawson, C., Kubatko, E.J., Westerink, J.J. and Bunya, S. (2011). “Implementation of a discontinuous Galerkin morphological model on two-dimensional unstructured meshes.” Comput.Methods Appl. Mech. Eng., 200, 189–207.

Papanicolaou, A. N., Elhakeem, M., Krallis, G., Prakash, S. and Edinger, J. (2008), “Sediment transport modeling review - current and future developments. ” J. Hydraul. Eng., 134, 1–14.

Pasquale, N., Perona, P., Schneider, P., Shrestha, J., Wombacher, A. and Burlando, P. (2011).“Modern comprehensive approach to monitor the morphodynamic evolution of a restored river corridor.” Hydrol. Earth Syst. Sci., 15, 1197–1212.F

Tassi, P.A., Rhebergen, S., and Vionnet, C. A. and Bokhove, O. (2008). “A discontinuous Galerkin finite element model for river bed evolution under shallow flows.” Comput. Methods Appl. Mech. Eng., 197, 2930–2947.

Toro, E. F. (2001). Shock-capturing methods for free-surface shallow flows, Wiley, Chichester, UK.

Toro, E. F., and García-Navarro, P. (2007). “Godunov-type methods for free-surface shallow flows: A review.” J. Hydraul. Res., 45(6), 736–751.

Toro, E. F., Spruce, M. and Speares, W. (1994). “Restoration of the contact surface in the HLL-Riemann solver.” Shock Waves., 4(1), 25–34.

Wu, W., Vieira, D. A., and Wang, S. S. Y. (2004).“One-dimensional numerical model for nonuniform sediment transport under unsteady flows in channel networks.” J. Hydraul. Eng., 130(9), 914–923.

Wu, W., and Wang, S. S. Y. (2007).“One-dimensional modeling of dam-break flow over movable beds.” J. Hydraul. Eng., 133(1), 48–58.

Wu, W. (2007). *“Computational River Dynamics”*, CRC Press.

Xia, J. Q., Lin, B. L., Falconer, R. A. and Wang, G. Q. (2010). "Modelling dam-break flows over mobile beds using a 2D coupled approach." Adv. Wat. Res., 33, 171–183.

Xing, Y., Zhang, X., and Shu, C.-W.(2010). "Positivity preserving high-order well-balanced discontinuous Galerkin methods for the shallow water equations." Adv. Water Resour., 33(12), 1476–1493.